Immunopathology and Infectious Diseases

Aberrant CD8+ T-Cell Responses and Memory Differentiation upon Viral Infection of an Ataxia-Telangiectasia Mouse Model Driven by Hyper-Activated Akt and mTORC1 Signaling

Anthony D. D'Souza,* Ian A. Parish,[†]
Sharen E. McKay,* Susan M. Kaech,[†‡]
and Gerald S. Shadel*[§]

From the Departments of Pathology, Immunobiology,[†] and Genetics,[§] Yale University School of Medicine, New Haven; and the Howard Hughes Medical Institute,[‡] Yale University School of Medicine, New Haven, Connecticut*

Immune system-related pathology is common in ataxia-telangiectasia (A-T) patients and mice that lack the protein kinase, A-T mutated (ATM). However, it has not been studied how ATM influences immune responses to a viral infection. Using the lymphocytic choriomeningitis virus (LCMV) infection model, we show that ATM$^{-/-}$ mice, despite having fewer naïve CD8+ T cells, effectively clear the virus. However, aberrant CD8+ T-cell responses are observed, including defective expansion and contraction, effector-to-memory differentiation, and a switch in viral-epitope immunodominance. T-cell receptor-activated, but not naïve, ATM$^{-/-}$ splenic CD8+ T cells have increased ribosomal protein S6 and Akt phosphorylation and do not proliferate well in response to IL-15, a cytokine important for memory T-cell development. Accordingly, pharmacological Akt or mammalian target of rapamycin complex 1 (mTORC1) inhibition during T-cell receptor activation alone rescues the IL-15 proliferation defect. Finally, rapamycin treatment during LCMV infection *in vivo* increases the number of memory T cells in ATM$^{-/-}$ mice. Altogether, these results show that CD8+ T cells lacking ATM have hyperactive Akt and mTORC1 signaling in response to T-cell receptor activation, which results in aberrant cytokine responses and memory T-cell development. We speculate that similar signaling defects contribute to the immune system pathology of A-T, and that inhibition of Akt and/or mTORC1 may be of therapeutic value. (Am J Pathol 2011, 178:2740–2751; DOI: 10.1016/j.ajpath.2011.02.022)

Ataxia-telangiectasia (A-T) is a human disease caused by mutations in the gene encoding the PI3-kinase-like protein kinase A-T mutated (ATM).[1] A-T is a multifaceted disease with complex pathology. Cerebellar degeneration underlies the hallmark ataxia symptoms, but another prominent issue is immune system-related pathology, including immunodeficiency and lymphoid cancers.[2] A-T patients commonly acquire hematological malignancies (eg, leukemia and lymphoma) that together with recurrent bronchial infections account for most of the mortality from the disease.[3] *ATM* gene knock-out mouse models of A-T exhibit many features of the human disease,[4–6] including sexual immaturity, immune system defects, hematopoietic stem cell defects, and thymic lymphoma, the latter of which is the most common cause of death in these animals.[4,7]

Immunodeficiency associated with decreased production of immunoglobulins A, E, and G2, and thymic hypoplasia has been documented in A-T patients.[8,9] The latter involves decreased peripheral CD4+ and CD8+ T-lymphocyte pools resulting from developmental defects in the thymic microenvironment.[9] Because ATM is recruited to double-strand breaks, it is likely that defects in the V(D)J recombination process, which results in a block in differentiation at the CD4+/CD8+ double-positive stage in the thymus, cause lower thymic output of mature CD4+ and CD8+ cells. This is corroborated by the ability of a functional T-cell receptor (TCR)-$\alpha\beta$ transgene to rescue the deficit in peripheral T cells in ATM$^{-/-}$ mice.[10] Despite

the defective thymic development of T cells in A-T patients, the immune function of mature T cells has been reported to be essentially normal.[11] However, to date, there have been no studies of how deficiency of ATM affects the response to an infection in A-T patients or in the mouse models of the disease.

The best-defined role for ATM is in the nuclear DNA damage response[2,12]; however, other functions for ATM have been described.[12,13] For example, ATM is important for mitochondrial homeostasis,[14,15] insulin signaling,[13,16] phosphorylation of 5'-AMP-activated protein kinase (AMPK),[17–19] and activation of Akt.[16,20] In addition, ATM signals to TSC2 in response to reactive oxygen species,[21] to inhibit mammalian target of rapamycin complex 1 (mTORC1) that itself is regulated by AMPK and Akt.[22–24] Finally, treatment of mice with the mTORC1 inhibitor rapamycin significantly increases the life span of *ATM*$^{-/-}$ mice by delaying development of thymic lymphoma.[25] Altogether, these results highlight how the loss of ATM might disrupt the integration of signals that feed into the nutrient-sensing mTORC1 pathway.

The CD8$^+$ T-cell response is a crucial arm of the adaptive immune system. In response to an infection, these cells are activated through the TCR, proliferate, and differentiate into cytotoxic effector cells that kill infected cells. Most of these cells die after clearance of the pathogen, but a subpopulation survives, loses effector cell properties, and become memory T cells.[26,27] Memory T cells are important for fighting recurrent infections, as they are programmed to respond faster and more effectively to the pathogen. The CD8$^+$ T-cell response to infection involves differentiation into short-lived effector cells and memory-precursor cells[26,28] that can be monitored based on surface expression of KLRG1 and CD127 markers. Effector CD8$^+$ T cells are preferentially represented in the KLRG1^{hi} population,[29,30] whereas cells that are CD127^{hi}, which is the receptor for IL-7, and KLRG1^{lo} preferentially become long-lived memory T cells.[31–33]

The response of CD8$^+$ T cells to TCR activation and the pathways involved in effector and memory cell differentiation are well-documented.[34] These include roles of the AMPK and mTORC1 pathways at several levels. For example, TCR activation leads to rapid activation of AMPK in response to Ca^{2+} signaling, presumably in anticipation of the enormous energy demand required for T-cell expansion.[35] In addition, we have shown that AMPK/mTORC1 signaling dynamically regulates mitochondrial biogenesis during TCR activation.[36] Finally, treatment of mice with the AMPK activator metformin or the mTORC1 inhibitor rapamycin enhances memory T-cell differentiation by boosting fatty acid oxidation.[33,37] Similarly, mTORC1 regulates differentially effector and memory T-cell commitment,[38] and it is a negative regulator of memory T-cell differentiation in mice.[33,37,39]

The goal of this study was to determine how loss of ATM affects normal CD8$^+$ T-cell activation and differentiation upon viral infection and to understand how alterations in mTORC1 and related pathways due to lack of ATM might contribute to the immune-related pathology of A-T using *ATM*$^{-/-}$ mice as a model of the disease and the well-characterized murine lymphocytic choriomeningitis virus (LCMV) infection paradigm.

Materials and Methods

Mice and Viral Infections

The wild-type (*ATM*$^{+/+}$) and *ATM*$^{-/-}$ mice (129SvEV background) were generated by crossing inbred heterozygous *ATM*$^{+/-}$ mice (obtained from the Howard Mount, University of Toronto) and were maintained according to approved Institutional Animal Care and Use Committee protocols. Genotyping was performed according to the PCR conditions outlined by the Jackson laboratory (Bar Harbor, ME). For LCMV infection studies, 4-week-old mice were infected with 2 × 10^5 *Pfu* LCMV-Armstrong (i.p.) as described.[40] Viral titers were measured by a plaque assay as described.[41] Rapamycin treatment in *ATM*$^{+/+}$ and *ATM*$^{-/-}$ animals was performed by the protocol of Araki et al.[33] For CD8$^+$ T-cell analyses from blood, infected mice were bled via retro-orbital bleeding procedure prescribed by Yale Animal Resources Center, and total blood cells were isolated after processing the blood by lysing the red blood cells using 0.83% ammonium chloride. Cells were processed and analyzed by fluorescence-activated cell sorting (FACS).

TCR Activation and Cytokine Culturing of T Lymphocytes in Vitro

For *in vitro* experiments, fresh spleens from 10-week-old mice were taken and total lymphocytes were prepared after lysing the red blood cells osmotically with 0.83% NH$_4$Cl buffer for 2 minutes. Cells (1 × 10^5) were seeded in individual wells of 96-well plates coated with 10 μg/mL anti-CD3 and anti-CD28 antibodies in 1 × PBS overnight at 4°C. When required, CD8$^+$ T lymphocytes were purified using CD8-positive miltenyi magnetic beads according to the manufacturer's instructions (Miltenyi Biotec Inc., Auburn, CA). For IL-2 or IL-15 treatments, 2.5 × 10^4 or 1 × 10^5 CD8$^+$ T lymphocytes that were TCR activated for 72 hours were cultured in 12-well tissue culture plates coated with 10 pg/mL mouse IL-2 or IL-15 (eBioscience, San Diego, CA). After 36 hours, 10 ng/mL IL-2 or IL-15 was added to ensure constant exposure to the cytokines. Where indicated, 10 nmol/L triciribine (Enzo Life Sciences International, Inc., Plymouth Meeting, PA) or 10 nmol/L rapamycin (Sigma-Aldrich, St. Louis, MO) were added during the TCR activation stage or cytokine stage, or both. During TCR activation, the drugs were provided twice, first at 24 hours and second at 48 hours to ensure constant drug action on all cells. The concentrations used were determined from pilot experiments aimed at finding doses that do not affect proliferation during TCR in both wild-type and *ATM*$^{-/-}$ CD8$^+$ T cells. Drug vehicle controls were always performed in parallel. Cells were stained with 0.4% trypan blue and the live cells were counted microscopically using a hemocytometer.

FACS Analyses

For intracellular staining with phospho-S6-alexafluor 433, tumor necrosis factor-α, IL-2 or interferon-γ, 1×10^6 CD8$^+$ T cells, or total splenocytes were fixed and permeabilized using the BD Cytofix/Cytoperm kit (BD Biosciences, San Jose, CA). Surface staining with different markers was performed using appropriate dilutions of antibodies, either as a cocktail or individually in 1× PBS buffer containing 0.5% fetal calf serum. Cells were incubated at 4°C or on ice for 20 minutes, washed three times in 1× PBS, and were then re-suspended in 1× PBS containing 0.1% fetal calf serum. For assaying cell death by FACS, cells were stained with propidium iodide according to the instructions using the BD AnnexinV/PI staining kit and assayed by FACS. The FACS analysis was performed using either a BD FACS Calibur or BD LSRII (Yale Cell Sorter Core Facility, New Haven, CT) and the data were analyzed using FlowJo software (Tree Star, Inc, Ashland, OR). Median fluorescence intensities were used for comparative analyses. Prism software was used to plot graphs and for statistical analyses. The mean ± SD was determined from at least three biological replicate samples and P values, which were determined using unpaired two-tailed student's t-test; they are indicated when appropriate in the figures, with values ≤0.05 interpreted as statistically significant.

Immunoblotting

Whole-cell protein extracts were prepared as follows: CD8$^+$ T cells (5×10^6) were lysed in 40 to 50 μL cold lysis buffer [50 mmol/L Tris–HCl, pH 8.8, 150 mmol/L NaCl, 0.5% Tween 20, 0.5% Triton-X 100, 0.1% SDS, 2 mmol/L EDTA, 10% glycerol, 1 × complete mini, EDTA free protease inhibitor cocktail (Roche Diagnostics, Indianapolis, IN), 1× phosphatase inhibitor cocktail II (AG Scientific, San Diego, CA)] at 4°C for 2 hours with careful pipetting once every 15 to 20 minutes. The resulting cell lysate was centrifuged at 13,000 rpm for 10 minutes and the soluble extract was analyzed after the protein concentration was determined using a Bio-Rad protein assay kit (Bio-Rad Laboratories, Hercules, CA).

Protein (20 μg) prepared as previously described was separated on 10% SDS polyacrylamide gels and then transferred electrophoretically to polyvinylidene difluoride membranes. Membranes were then blocked with 5% bovine serum albumin/TBST (10 mmol/L Tris–HCl, pH 8.0, 150 mmol/L NaCl, 0.05% Tween 20) for 30 minutes and then incubated with the desired primary antibody (in 5% bovine serum albumin/TBST) overnight at 4°C. Blots were rinsed five times with 1× TBST for 5 minutes and then incubated with the corresponding secondary antibody (5% bovine serum albumin/TBST) at 4°C for 1 hour. Blots were then washed five times for 10 minutes with TBST, and the cross-reacting proteins were visualized using the Western Lighting chemiluminescence reagent plus kit (Perkin-Elmer LAS, Inc., Waltham, MA) to expose X-ray film. Exposed films were developed and imaged with Bio-Rad VersaDoc using Quantity One software (Bio-Rad Laboratories). For serial Western blots, the membrane was stripped using Restore

TM Western blot stripping buffer (Pierce, Rockford, IL) and probed again as previously described.

The antibodies used for the Western analysis were as follows: acetyl-CoA carboxylase or ACC (#3662), pSer79 ACC (#3661), pThr172-AMPK (#2535), AMPK (#2603), S6 (#2217), pSer235 S6 (#4858S), phosphatase and tensin homolog (PTEN) (#9559), phospho-PTEN (#9554S), pSer473 Akt (#4060S), pThr308 Akt (#9275S), and Akt (#9272), all purchased from Cell Signaling (Danvers, MA). Anti-actin antibody (A5060) from Sigma was used as a loading control. All primary antibodies were used at a 1:1000 dilution. Horse-radish peroxidase (HRP)-conjugated secondary antibodies, donkey anti-rabbit IgG (sc-2313), and goat anti-mouse (sc-2314) were purchased from Santa Cruz Biotechnology (Santa Cruz, CA) and were used at a 1:10,000 dilution.

Results

ATM$^{-/-}$ Mice Have Reduced Antiviral CD8$^+$ T-Cell Responses to LCMV Infection

Before taking advantage of the LCMV infection model system, we ascertained differences in T cell populations in uninfected ATM$^{-/-}$ and age-matched, wild-type (ATM$^{+/+}$), littermate control mice. The majority of ATM$^{-/-}$ mice from our strain succumb to malignant thymic lymphoma within 15 to 20 weeks. At 10 weeks, we found that based on the distribution of the four populations of thymic T cells (CD4$^+$ CD8$^+$, double-positive; CD4$^-$ CD8$^-$, double-negative; CD4$^+$ CD8$^-$, CD4 single-positive; CD4$^-$ CD8$^+$, CD8 single-positive) ATM$^{-/-}$ mice had fewer total thymocytes than the control, wild-type animals, a greater percentage of double-positive, and a deficit in both single-positive populations (see Supplemental Figure S1 at *http://ajp.amjpathol.org*). Some of the ATM$^{-/-}$ mice had a twofold to threefold increase in total thymocytes compared to the control wild-type mice, nearly all of which were double-positive, indicating the beginning stages of thymic lymphoma development.[5,25] As previously reported,[9] our ATM$^{-/-}$ mice also had deficits in total splenocytes, CD8$^+$ T lymphocytes, and CD4$^+$ T lymphocytes (see Supplemental Figure S1B at *http://ajp.amjpathol.org*).

To avoid complications from double-positive proliferation and thymic lymphoma, we infected 4-week-old ATM$^{-/-}$ and age-matched wild-type littermate control mice with LCMV-Armstrong and monitored their response weekly for 6 weeks following viral infection. Before infection the ATM$^{-/-}$ mice had fewer splenocytes, CD8$^+$ T cells, and CD4$^+$ T cells in the spleen (Figure 1, A–C). Likewise, CD8$^+$ T cells were also depleted in blood, yet they had normal expression of markers of activated T cells (see Supplemental Figure S2 at *http://ajp.amjpathol. org*). At postinfection day 8, we observed typical expansion of total splenocytes, CD8$^+$, and CD4$^+$ T cells (Figure 1, A–C), as well as viral-specific CD8$^+$ T cells (Figure 1D), coincident with elimination of LCMV (no virus in the blood at postinfection day 8) in the wild-type mice. This was followed by a typical contraction of these same cells types in wild-type mice measured at postinfection day 41 (Figure
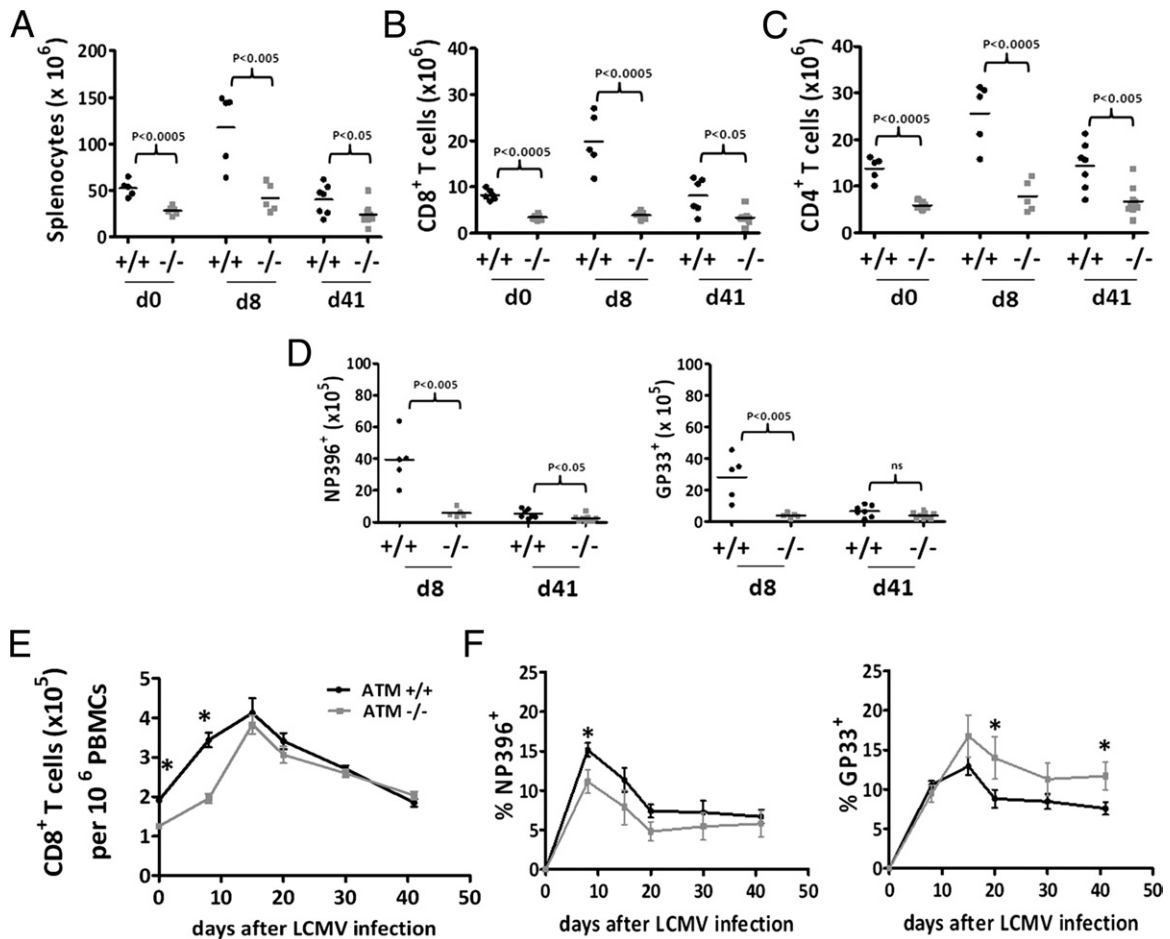
Figure 1. Fewer splenic T cells and altered immunodominance hierarchy in CD8$^+$ T cells in ataxia-telangiectasia mutated *(ATM)*$^{-/-}$ mice in response to lymphocytic choriomeningitis virus (LCMV) infection. **A:** Total splenocytes in wild-type *ATM*$^{+/+}$ (black circles in **A–D**) and *ATM*$^{-/-}$ (grey squares in **A–D**) mice at day 0 (d0), day 8 (d8), and day 41 (d41) post-LCMV infection. **B:** Total splenic CD8$^+$ T cells at d0, d8, and d41 after post-LCMV infection *ATM*$^{+/+}$ and *ATM*$^{-/-}$ mice. **C:** Total splenic CD4 T cells at d0, d8, and d41 post-LCMV infection of *ATM*$^{+/+}$ and *ATM*$^{-/-}$ mice. **D:** Total D^{b}NP396-CD8+ and D^{b}GP33-CD8+ T cells at d8 and d41 post-LCMV infection in *ATM*$^{+/+}$ and *ATM*$^{-/-}$ mice, respectively. **E:** Total CD8$^+$ T cells in the blood (expressed as the number in 1×10^6 peripheral blood mononuclear cells (PBMCs) in wild-type and *ATM*$^{-/-}$ mice at d0, d8, day 15, day 20, day 30, and d41 post-LCMV infection. **F:** Percentage of D^{b}NP396-CD8+ and D^{b}GP33-CD8+ T cells at d0, d8, day 15, day 20, day 30, and d41 post-LCMV infection in wild-type and *ATM*$^{-/-}$ mice, respectively. **A–C:** 5 *ATM*$^{+/+}$ and 5 *ATM*$^{-/-}$ mice were analyzed in two separate experiments on d0; the combined data from two separate experiments is shown representing a total of 5 *ATM*$^{+/+}$ and 5 *ATM*$^{-/-}$ mice analyzed on d8 postinfection and a total of 7 *ATM*$^{+/+}$ and 8 *ATM*$^{-/-}$ mice analyzed on day 41 postinfection from two separate experiments. For blood analyses in data from E and F, 10 *ATM*$^{+/+}$ and 9 *ATM*$^{-/-}$ mice were analyzed in two independent experiments. Statistically significant differences are indicated directly or by **asterisks**, which represent *P* values from an unpaired *t*-test of <0.05.

1, A–D). However, the response in *ATM*$^{-/-}$ mice was markedly different. First, at day 8, the total number of splenocytes (Figure 1A), and CD8$^+$ and CD4$^+$ T cells (Figure 1, B and C) were substantially reduced compared to the wild-type mice, no doubt stemming, at least in part, from the T-cell lymphopenia before infection. Second, both the expansion (comparing postinfection day 8 with day 0) and contraction (comparing postinfection day 41 with day 8) of all these cell types was blunted significantly compared to that in wild-type mice. In the end, the number of viral-specific CD8$^+$ T cells at postinfection day 41 was twofold to threefold lower in *ATM*$^{-/-}$ mice (Figure 1D).

Next, we examined the response of viral-specific CD8$^+$ T cells in the blood and found that the overall frequency of CD8$^+$ T cells in the *ATM*$^{-/-}$ mice lagged behind that in wild-type mice during the first 2 weeks postinfection, but eventually caught up (Figure 1E). We also observed a change in the LCMV immunodominance hierarchy in the *ATM*$^{-/-}$ mice. That is, the percentage

of the most immunodominant T-cell population, the D^{b}NP$_{396-404}$$^+$ LCMV-specific CD8$^+$ T cells, was also considerably reduced in the blood of ATM-deficient mice relative to wild-type during the first 3 weeks after infection (Figure 1F, left panel). However, the frequency of a more subdominant T-cell population in wild-type mice, the D^{b}GP$_{33-41}$$^+$ LCMV-specific CD8$^+$ T cells, were comparable, if not higher, at all time points examined in the *ATM*$^{-/-}$ mice (Figure 1F, right panel). Thus, the normally subdominant GP$_{33-41}$-specific CD8$^+$ T-cell response was enhanced in the *ATM*$^{-/-}$ mice. Similar relative immunodominance relationships were observed when viral-specific splenic CD8$^+$ T cells were compared (Figure 1D).

Altogether, these results show that ATM is required for optimal formation of virus-specific effector CD8$^+$ T cells during an acute viral infection and the normal response to epitopes. Furthermore, our results implicate a combination of effects are responsible for these T-cell phenotypes, including a lower number of CD8$^+$ T cells preinfec-
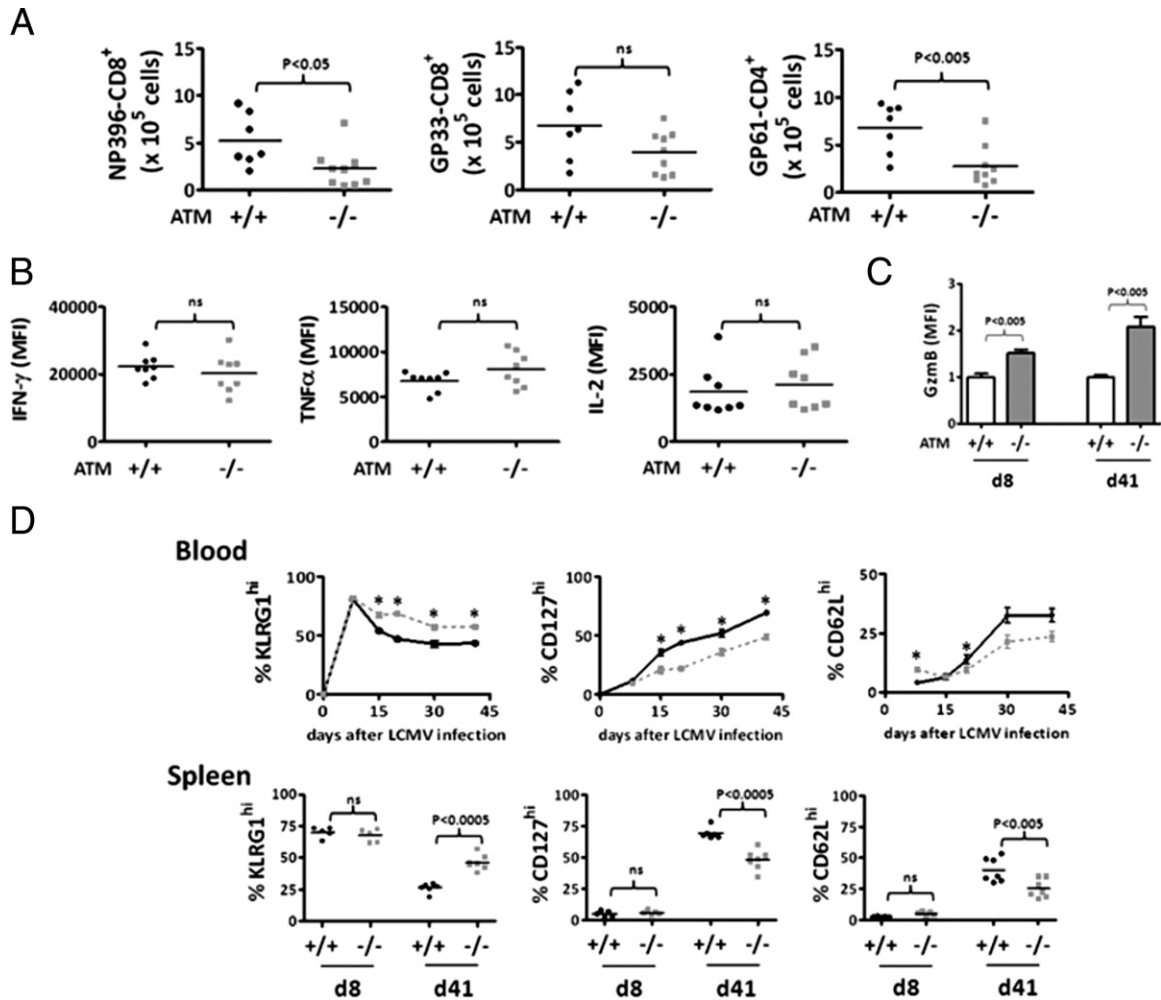
A

B

C

D

Figure 2. Defective memory CD8^{+} T-cell differentiation ataxia-telangiectasia mutated *(ATM)*[−/−] mice post-LCMV infection. **A:** Number of viral specific D[b]NP396-CD8+, D[b]GP33-CD8+ and D[b]GP61-CD4+ memory T cells in spleens from *ATM*^{+/+} and *ATM*^{−/−} mice at day 41 after lymphocytic choriomeningitis virus (LCMV) infection. **B:** Comparison of median fluorescence intensities (MFI) obtained from fluorescence-activated cell sorting (FACS) analyses of intracellular staining of interferon-γ, tumor necrosis factor-α, and IL-2 of D[b]GP33-CD8 T cells from *ATM*^{+/+} and *ATM*^{−/−} mice at day 41 postinfection. **C:** Relative intracellular expression of granzyme B (GzmB) in D[b]GP33-CD8+ T cells from in *ATM*^{+/+} and *ATM*^{−/−} mice at days 8 and 41 postinfection. The MFI from wild-type cells was given a value of 1.0 for normalization of the results. **D: Top row,** percent KLRG1^{hi}, CD127^{hi}, and CD62L^{hi} D[b]GP33-CD8+ T cells at days 8, 15, 20, 30, and 41 in the blood of LCMV-infected *ATM*^{+/+} (bold black line) and *ATM*^{−/−} (dashed gray line) mice. **Bottom row,** percent KLRG1^{hi}, CD127^{hi}, and CD62L^{hi} D[b]GP33-CD8+ T cells at days 8 and 41 post-LCMV infection for *ATM*^{+/+} (black circles) and *ATM*^{−/−} (grey squares) mice are shown. Whereas for the blood, the combined data from two separate experiments representing 7 *ATM*^{+/+} and 9 *ATM*^{−/−} mice are shown, and for the spleen, the combined data from separate experiments representing 5 pairs of wild-type and *ATM*^{−/−} mice on day 8 and 7 wild-type and 9 *ATM*^{−/−} mice on day 41 are shown. Statistically significant differences are indicated directly or by **asterisks**, which represent *P* values from an unpaired *t*-test of <0.05.

tion and altered expansion/contraction dynamics in response to the viral infection. Despite these demonstrable defects, *ATM*^{−/−} mice were capable of clearing LCMV effectively.

Abnormal Memory CD8^{+} T-Cell Development and Decreased Formation of T_{CM} Cells in the Absence of ATM

Next, we examined the development of memory CD8^{+} T cells after LCMV infection and found that the total number of LCMV-specific memory CD8^{+} and CD4^{+} T cells that formed was about twofold lower in the absence of ATM (Figure 2A). Despite this reduction in overall memory T-cell number, the percentage of total and viral-specific memory CD8^{+} T cells in the spleen of *ATM*^{−/−} mice was comparable,

albeit moderately reduced, to that in wild-type mice. As observed in the blood, dominance of the GP$_{33-41}$-specific CD8^{+} T-cell response was observed in splenic memory CD8^{+} T cells in *ATM*^{−/−} animals (see Supplemental Figure S3 at *http://ajp.amjpathol.org*).

The memory CD8^{+} T cells that did form in the absence of ATM were functional, producing similar amounts of interferon-γ, tumor necrosis factor-α and IL-2 as wild-type cells when reactivated *in vitro* (Figure 2B). However, the expression of granzyme B (a potent cytotoxic molecule) was noticeably increased in the ATM-deficient CD8^{+} T cells relative to the wild-type cells at both days 8 and 41, which represent effector and memory time points, respectively (Figure 2C). This suggested that the memory CD8^{+} T cells were in a more "effector-like" state, as opposed to a resting memory state, which prompted us to more closely compare

the types of memory CD8$^+$ T cells that formed in the absence of ATM. During LCMV infection in wild-type mice, the majority of effector cells generated are terminally differentiated cells that do not persist long term after infection.[29,32] These end-stage effector cells express high amounts of an inhibitory receptor KLRG1 and low amounts of the IL-7Rα (CD127), which is associated with memory CD8$^+$ T cell survival.[42] In contrast, a smaller subset of effector cells develop into "memory precursor cells" that preferentially survive after infection and can be distinguished by the inverse expression pattern of KLRG1 and IL-7Rα (ie, these cells are KLRG1^{lo} CD127^{hi}).[40,43] Thus, as memory CD8$^+$ T cells form and mature, the frequency of KLRG1^{lo} CD127^{hi} cells increases with time. Moreover, "central" memory (T$_{CM}$) CD8$^+$ T cells, which can be distinguished from "effector" memory (T$_{EM}$) CD8$^+$ T cells by increased expression of CD62L, also gradually accumulate with time.[43] T$_{CM}$ cells home to lymphoid organs and have higher proliferative (and often protective) capacity on re-infection relative to CD62L^{lo} T$_{EM}$ CD8$^+$ T cells.[43,44]

We found that initially the formation of LCMV-specific terminally differentiated (KLRG1^{hi} CD127^{lo}) and memory precursor (CD127^{hi} KLRG1^{lo}) effector cells was very similar between wild-type and $ATM^{-/-}$ mice in both the blood and the spleen (Figure 2D). However, at later time points in the blood (ie, days 15 through 41 postinfection), the antiviral CD8$^+$ T-cell population in $ATM^{-/-}$ mice contained a substantially larger percentage of KLRG1^{hi} CD8$^+$ T cells than the wild-type animals (Figure 2D, left panel). Consequently, fewer CD127^{hi} KLRG1^{lo} and CD62L^{hi} (T$_{CM}$) memory CD8$^+$ T cells accumulated in the $ATM^{-/-}$ mice (Figure 2D, right two panels). On day 41, $ATM^{-/-}$ mice also showed accumulation of a larger percentage of KLRG1^{hi} and fewer CD127^{hi} KLRG1^{lo} and CD62L^{hi} (T$_{CM}$) memory CD8$^+$ T cells in spleen (Figure 2D). Together these data show that ATM-deficiency impairs the maturation of memory CD8$^+$ T cells, accompanied by a preferential maintenance of GzmB$^+$ KLRG1^{hi} CD127^{lo} CD62L^{lo} T$_{EM}$ cells.

$ATM^{-/-}$ CD8$^+$ T Cells Exhibit a Proliferation Defect in Response to IL-15

To probe the nature of the effector to memory differentiation phenotype we elucidated in $ATM^{-/-}$ mice *in vivo*, we activated splenic CD8$^+$ T cells *in vitro* with IL-2, a potent T-cell mitogen, or IL-15, a cytokine required for memory T-cell proliferation and maintenance *in vivo*. This approach has been shown by others to skew the CD8$^+$ T cells toward T$_{EM}$- and T$_{CM}$- as with phenotypes, respectively,[45,46] and consists of two primary phases in which the T cells are first activated via their TCR for 3 days, followed by 3 days of culture with IL-2 or IL-15 (Figure 3A). We confirmed this through our own analysis of the effects of IL-2 and IL-15 under these conditions on the memory cell markers, CD127, and CD62L (see Supplemental Figure S4 at *http://ajp.amjpathol.org*). After treatment with IL-15, a significant proliferation defect was observed in the $ATM^{-/-}$ CD8$^+$ T cells, whereas no such defect was observed in cells treated with IL-2 (Figure 3B). Neither cytokine treatment resulted in significant cell death to confound the experiment (Figure 3E). Thus, ATM-deficient CD8$^+$ T cells are specifically

impaired in responding and proliferating to IL-15, a critical cytokine for T$_{CM}$ memory CD8$^+$ T-cell homeostasis.[46,47]

TCR-Activated $ATM^{-/-}$ CD8$^+$ T Cells Sustain Activated Akt Phosphorylation after IL-15, Treatment, and Inhibition of Akt during TCR Activation Restores Proliferation in Response to IL-15

One major pathway that is downstream of IL-2 and IL-15, and affects terminal effector cell and T$_{EM}$ formation in CD8$^+$ T cells *in vivo* is the nutrient-sensing PI3K/Akt/mTORC1 pathway.[33,37,39,45,48,49] Additionally, under certain conditions, ATM regulates AMPK, an inhibitor of mTORC1.[17–19] Therefore, we probed the activity of these pathways by Western blot in $ATM^{-/-}$ CD8$^+$ T lymphocytes treated with IL-15 after TCR activation. Compared to wild-type CD8$^+$ T cells, we observed a significant increase in Akt phosphorylation (both T308 and S473) (Figure 3C) in the $ATM^{-/-}$ CD8$^+$ T cells, and this was associated with increased inhibitory phosphorylation (S380/T382/383) of PTEN. Unexpectedly, this hyper-Akt activity did not correlate with increased phosphorylation of the mTORC1 substrate S6 (Figure 3C), indicating that CD8$^+$ T cells lacking ATM have elevated Akt, but not mTORC1 activity. Indeed, ATM-deficient CD8$^+$ T cells had increased AMPK activity as demonstrated by hyper-phosphorylation of AMPK at T172 and its substrate ACC S79 (Figure 3C). These results suggest that ATM is necessary to properly integrate signals from Akt and AMPK to mTORC1. In the T-cell context described herein, the loss of this function apparently results in decreased PTEN activity and increased AMPK activity, the net result of which is hyper-Akt signaling, without subsequent activation of mTORC1.

Because enhanced Akt activation was observed in IL-15 cultured CD8$^+$ T lymphocytes, we tested the hypothesis that inhibition of Akt would rescue the proliferation defect in response to IL-15. When the Akt inhibitor triciribine was added, either during TCR activation alone or during both phases (TCR stimulation and IL-15 treatment), IL-15-driven proliferation in $ATM^{-/-}$ cells was considerably augmented (Figure 3D), despite similar increases in cell death in the triciribine-treated cultures for both wild-type and $ATM^{-/-}$ cells (Figure 3E). Proliferation of wild-type cells was also enhanced by triciribine treatment during TCR activation alone (Figure 3D, compare left and middle bars), but not to the same degree as the $ATM^{-/-}$ cells. These results indicate that hyperactivation of Akt in the $ATM^{-/-}$ condition (and also in wild-type CD8$^+$ T cells to a significant degree) impairs T-cell proliferation in response to IL-15, and this is rescued by reducing Akt activity.

Inhibition of mTORC1 Signaling Pathway during TCR Activation Rescues IL-15 Proliferation Defect of $ATM^{-/-}$ CD8$^+$ T Cells

The ability of Akt inhibition during TCR activation alone to rescue the IL-15 proliferation defect of $ATM^{-/-}$ CD8$^+$ T cells (Figure 3B, compare left and middle bars) suggested that active Akt signaling before or during TCR activation could lead to subsequent effects on IL-15-driven proliferation. To address

this directly, we analyzed PI3K/Akt/mTORC1 and AMPK signaling events before and during TCR activation (Figure 4A). Western blot analysis of TCR-activated $ATM^{-/-}$ cells revealed that Akt was hyperphosphorylated compared to identically treated wild-type cells, as in IL-15-treated cells, albeit to a lesser extent than seen after IL-15 treatment (compare Figures 3C and 4A). However, before TCR activation, $ATM^{-/-}$ CD8$^+$ T cells had either normal or hypophosphorylated Akt, suggesting that Akt was hyperactivated in $ATM^{-/-}$ cells only after TCR activation (Figure 4A). The major difference observed in the TCR-activated $ATM^{-/-}$ CD8$^+$ T cells was considerable up-regulation of mTORC1 signaling (as measured by S6 phosphorylation) (Figure 4A), a difference that was not observed prior to TCR activation. Next, we followed the kinetics of S6 phosphorylation (using flow cytometry) as a readout of mTORC1 signaling during the first 24, 48, and 72 hours after TCR activation (Figure 4B). $ATM^{-/-}$ T cells exhibited a similar degree of up-regulation S6 phosphorylation as wild-type cells at 24 and 48 hours, but were deficient in down-regulating mTORC1 at later points (eg, 72 hours) after TCR activation *in vitro* (Figure 4B). Similarly, S6 phosphorylation was increased

in $ATM^{-/-}$ CD8$^+$ T cells at day 8 post-LCMV infection *in vivo* (Figure 4C). Based on these data, we then hypothesized that another reason Akt inhibition during TCR activation is able to rescue the IL-15 proliferation defect in $ATM^{-/-}$ cells (Figure 3D) is via down-regulation of the elevated mTORC1 activity during TCR activation. This was confirmed by the ability of the mTORC1 inhibitor rapamycin, like triciribine, to rescue the IL-15 proliferation defect of $ATM^{-/-}$ T cells when added just during TCR activation (Figure 4D). This rapamycin regimen did not result in significant differences in the cell death of two cell types (Figure 4E).

Rapamycin Treatment during LCMV Infection Improves Memory CD8$^+$ T-Cell Formation in ATM$^{-/-}$ Mice

Based on the fact that rapamycin treatment *in vitro* improves the ability of activated ATM-deficient CD8$^+$ T cells to respond to IL-15 (Figure 4D), and *in vivo* increases the percentage and number of KLRG1^{lo} CD127^{hi} CD62L^{hi}
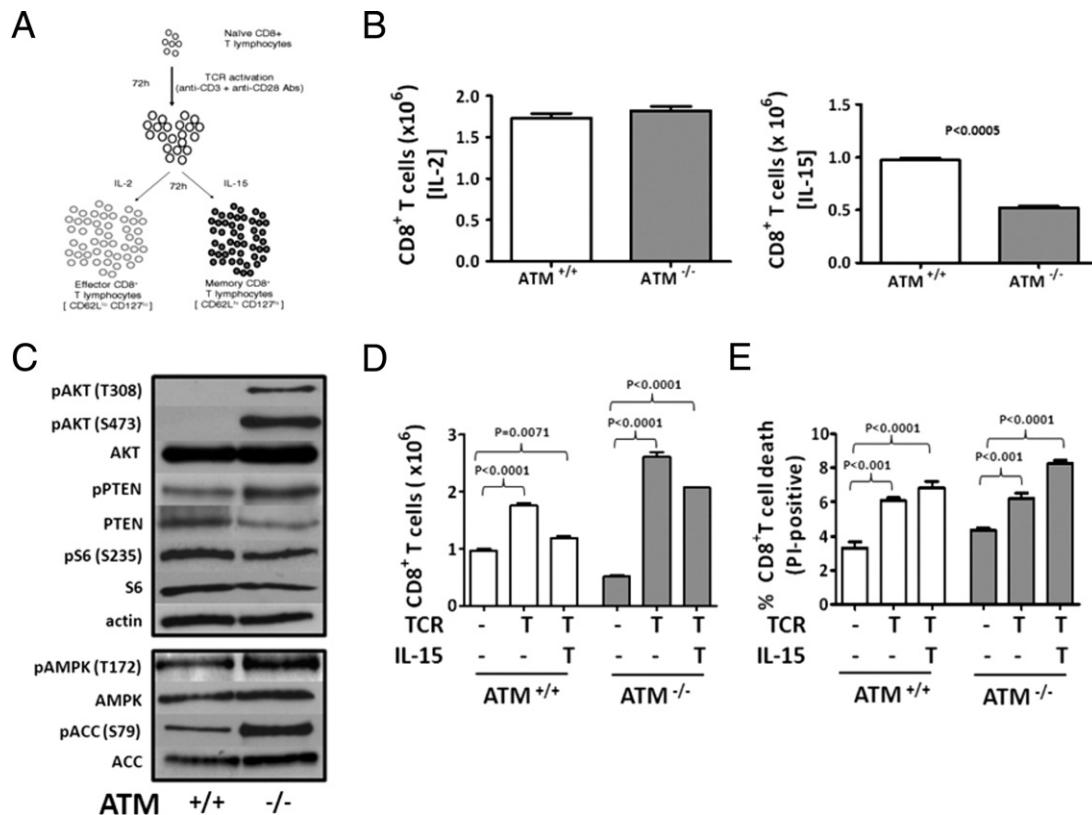

Figure 3. T-cell receptor (TCR)-activated ataxia-telangiectasia mutated (ATM)$^{-/-}$ CD8$^+$ lymphocytes sustain heightened Akt phosphorylation and exhibit a proliferation defect in response to IL-15 treatment that is rescued by the Akt inhibitor triciribine. **A:** Experimental scheme used to test the response of $ATM^{-/-}$ lymphocytes to IL-2 and IL-15, which after TCR activation (using anti-CD3 and anti-CD28 antibodies) skews the cell populations toward effector and memory phenotypes *in vitro*. **B:** Number of CD8$^+$ T cells after IL-15 (**right**) or IL-2 (**left**) treatment of $ATM^{+/+}$ and $ATM^{-/-}$ splenocytes, according to the scheme in **A**. For culturing in IL-2 and IL-15, the starting CD8$^+$ T-cell number was 2.5×10^4 and 1×10^5, respectively. The *P* value from a two-tailed unpaired *t*-test is indicated for the IL-15 experiment, and no difference was observed in the IL-2 experiment. **C:** Western blot analyses of phosphorylated Akt (S473, T308), PTEN (S380/T382/383), S6 (S235/236), AMPK (T172), and ACC (S79) and the corresponding unphosphorylated proteins in splenic CD8$^+$ T lymphocytes from wild-type and $ATM^{-/-}$ mice treated with IL-15 according to the scheme in **A**. Actin was used as the loading control. Similar results were obtained 3 times from different sets of mice. **D:** Total CD8$^+$ T cells from $ATM^{+/+}$ (open bars) or $ATM^{-/-}$ (filled bars) mice after IL-15 treatment according to the scheme, (**A**) with (+) or without (−) 10 nmol/L triciribine added at the stage indicated by T (ie, during TCR activation alone or during both TCR activation and IL-15 treatment). (**E**) Total percent CD8$^+$ T-cell death evaluated by propidium iodide (PI)-positive cells after IL-15 treatment according to the scheme (**A**), with (+) or without (−)10 nmol/L triciribine added at the stage indicated by T. Analysis of cells from $ATM^{+/+}$ (open bars) and $ATM^{-/-}$ (filled bars) mice are shown. **D** and **E:** The *P* value from a two-tailed unpaired *t*-test for the comparison of $ATM^{-/-}$ to $ATM^{+/+}$ without drug treatment is shown above the brackets, and those for comparisons of drug-treated to untreated within in each group/genotype are as indicated.
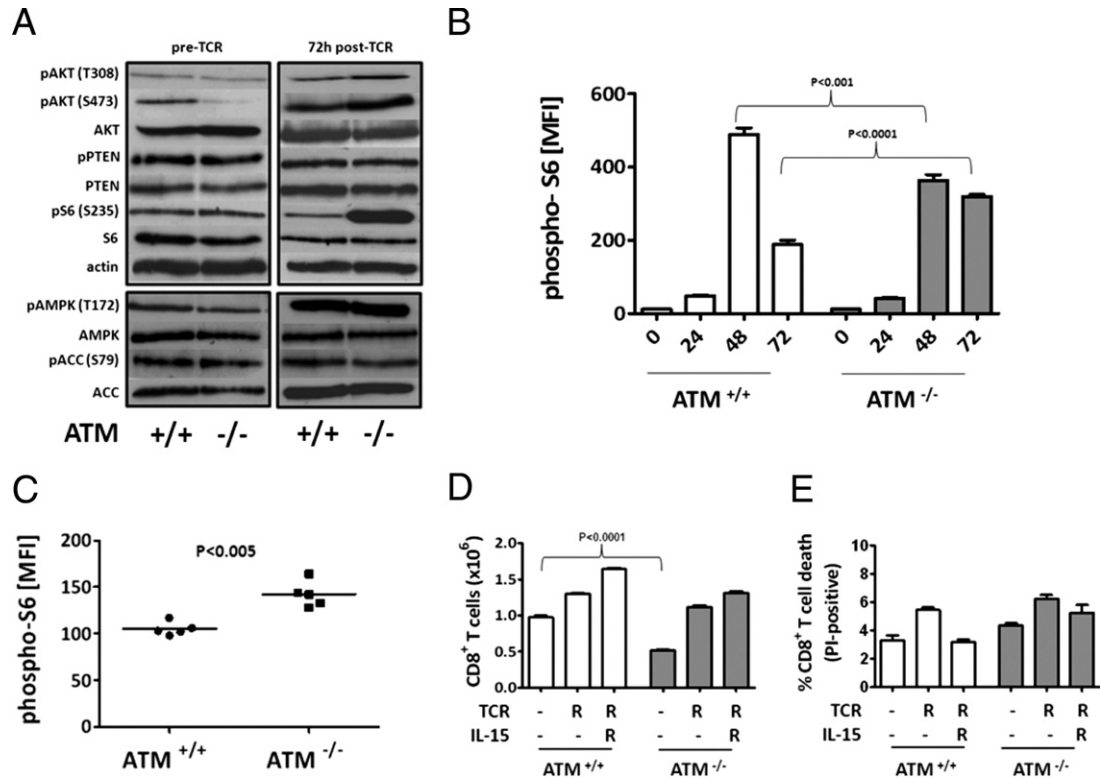
Figure 4. Rapamycin treatment during T-cell receptor (TCR) activation rescues the IL-15 proliferation defect in ataxia-telangiectasia mutated (ATM)$^{-/-}$ splenic CD8$^+$ T lymphocytes. **A:** Western blot analyses (as described in Figure 3C), except the $ATM^{+/+}$ and $ATM^{-/-}$ cells were collected before TCR stimulation (pre-TCR) and 72 hours after TCR activation (post-TCR) (as described in Figure 3A). **B:** Graphed are the median fluorescence intensities (MFI) from intracellular staining of phosphorylated ribosomal protein S6 (phospho-S6; S235/236) calculated from FACS plots of $ATM^{+/+}$ (white bars) and $ATM^{-/-}$ (gray bars) CD8$^+$ T cells before (at 0 hours), and at 24, 48, and 72 hours of TCR activation *in vitro*. **C:** Same as **B**, except the analysis of CD8$^+$ T cells on day 8 post-LCMV infection *in vivo* is shown. The data from 5 $ATM^{+/+}$ and 5 $ATM^{-/-}$ mice were analyzed. **D:** Total CD8$^+$ T cells from $ATM^{+/+}$ (open bars) or $ATM^{-/-}$ (filled bars) after IL-15 treatment, according to the scheme (**A**), with (+) or without (−) 10 nmol/L rapamycin added at the stage indicated by "R" (ie, during TCR alone or during both TCR activation and IL-15 treatment). **E:** Total percent CD8$^+$ T-cell death evaluated by propidium iodide (PI)-positive cells after IL-15 treatment, according to the scheme (**A**), with (+) or without (−) 10 nmol/L rapamycin added at the stage indicated by "R". Analysis of cells from $ATM^{+/+}$ (open bars) and $ATM^{-/-}$ (filled bars) mice are shown. **D** and **E:** The P value from a two-tailed unpaired *t*-test for the comparison of $ATM^{-/-}$ to $ATM^{+/+}$ without drug treatment is shown above the brackets, and those for comparisons of drug treated to untreated within each group/genotype are as indicated.

T$_{CM}$ CD8 T cells,[33] we hypothesized that $ATM^{-/-}$ mice might mount a better memory response if mTORC1 was inhibited during an LCMV infection. To test this hypothesis, we treated $ATM^{-/-}$ and wild-type mice with rapamycin starting 1 day before LCMV infection to postinfection day 8 and followed the kinetics of effector and memory T-cell formation in the blood at postinfection days 8 to 30. As previously reported in wild-type mice,[33] rapamycin treatment substantially decreased the frequency KLRG1^{hi} terminal effector cells and correspondingly increased the number of CD127^{hi} KLRG1^{lo} CD8$^+$ T cells formed postinfection (Figure 5A). Likewise, rapamycin treatment augmented the frequency of CD62L^{hi} T$_{CM}$ cells at 30 days postinfection (Figure 5A, right panel). Importantly, similar, albeit more modest, effects on these phenotypes were observed in the $ATM^{-/-}$ mice treated with rapamycin (Figure 5A; see also Supplemental Figure S5 at *http://ajp.amjpathol.org*). These results show that decreasing mTORC1 activity in $ATM^{-/-}$ mice can partially rescue the altered memory CD8$^+$ T-cell development in $ATM^{-/-}$ mice in response to LCMV infection.

Next, we examined the frequency of memory CD8$^+$ T cells in the blood that formed after rapamycin treatment. As previously reported,[33] rapamycin treatment of wild-type mice increased the frequency of LCMV-specific memory CD8$^+$ T cells that formed 30 days postinfection (Figure 5B). Interestingly, in the $ATM^{-/-}$ mice, rapamycin also significantly boosted the population of GP$_{33-41}$-specific CD8$^+$ T cells at postinfection day 15, but this effect was diminished by postinfection day 30 (Figure 5B). However, no effect of rapamycin treatment was observed in the NP$_{396-404}$-specific CD8$^+$ T-cell population (Figure 5B). These results suggest that inhibition of the mTORC1 signaling pathway during early CD8$^+$ T-cell activation can have beneficial effects in terms of the immune response to viral infections, but that they are not as long lasting as those seen in wild-type animals.

Discussion

Previous studies of A-T patients revealed mostly intact immune responses, although mild differences in T-lymphocyte function have been demonstrated in some cases.[11,50] Using $ATM^{-/-}$ mice as a model of human A-T immune dysfunction, we confirm that the primary immune response is indeed effective (Figure 2, B and C), and the mice are able clear an LCMV viral infection with similar
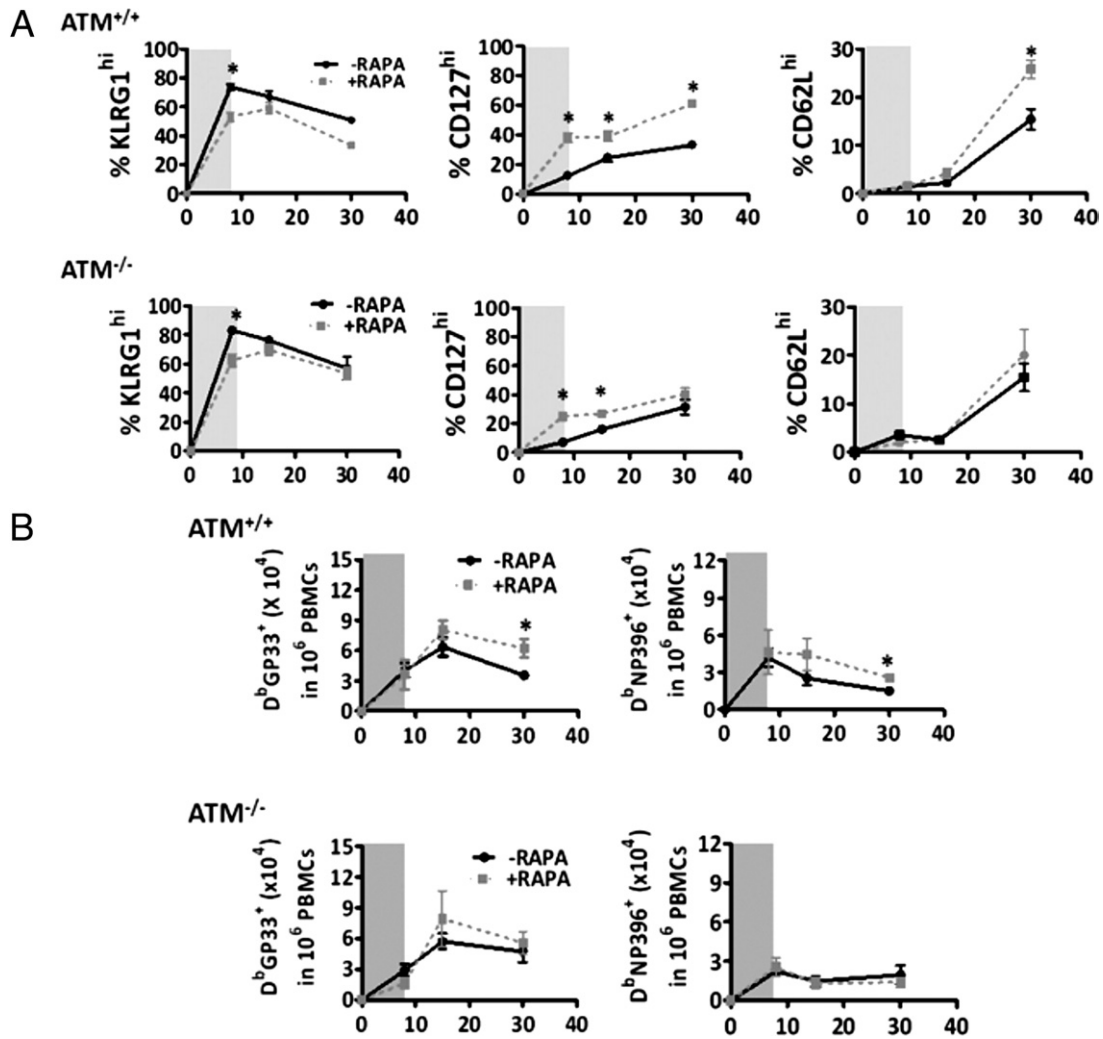
Figure 5. Rapamycin treatment during lymphocytic choriomeningitis virus infection improves memory CD8^{+} T-cell development in ataxia-telangiectasia mutated $(ATM)^{-/-}$ mice. **A:** Percent of KLRG1^{hi}, CD127^{hi}, and CD62L^{hi} D[b]GP33-CD8+ T cells in $ATM^{+/+}$ and $ATM^{-/-}$ mice at days 8, 15, and 30 post-LCMV infection with (dashed gray) or without (black line) rapamycin treatment between day −1 to day +8 (indicated by the gray shading). **B:** Same as in **A**, except total D[b]GP33+ and D[b]NP396+ CD8+ T lymphocytes were analyzed. Statistically significant differences are indicated by **asterisks**, which represent *P* values from an unpaired *t*-test of <0.05. PBMCs, peripheral blood mononuclear cells. X-axes denotes days after LCMV infection.

efficiency as wild-type mice. Nonetheless, viral T-cell responses and memory T-cell development are aberrant in the $ATM^{-/-}$ mice (Figures 1 and 2). These findings are potentially important from a clinical standpoint, because persistent effector T-cell function as a consequence of a viral infection, as our results indicate, can potentially cause inflammation. This could be relevant to the fact that A-T patients are predisposed to cancer and diabetes, both of which are influenced by inflammation.[3,51] In further support of this premise, persistent inflammation is a major factor that aggravates DSS-induced colitis in $ATM^{-/-}$ mice.[52]

A second phenotype we observed *in vivo* in response to LCMV infection is a switch in T-cell epitope immunodominance relationships in the $ATM^{-/-}$ mice (Figure 1F). Shifts in CD8^{+} T-cell immunodominance during early stages of LCMV infection are influenced by variability between epitope abundance and affinity, as well as frequency of precursor T-cell population.[53] Although we do not know how the lack of ATM causes this switch, given

that the NP396 epitope is the most abundant, it is tempting to speculate that the defects in signaling downstream of TCR we have identified in $ATM^{-/-}$ CD8^{+} T cells (Figure 4A) may dampen its normally strong TCR signal allowing the less abundant GP33 epitope to now compete more effectively. In addition, the reduced total number of viral-specific CD8^{+} T cells produced in the spleen of $ATM^{-/-}$ mice could influence the immunodominance phenotype observed in blood (Figure 1D–1F). We speculate that such alterations in epitope response, coupled with the production of fewer viral-specific memory T cells (Figure 1D), if recapitulated in human A-T patients, could result in susceptibility to secondary infections.

Moving from our characterization of CD8^{+} T-cell responses to LCMV infection in the $ATM^{-/-}$ mice to *in vitro* models of memory cell differentiation allowed us to uncover other important defects in $ATM^{-/-}$ CD8^{+} T cells. Specifically, we found that TCR-activated $ATM^{-/-}$ splenocytes have a significant proliferation defect in response to IL-15 (Figure 3B), a regimen that has been

used by others to induce a population of cells with memory T-cell-like properties.[45] This was accompanied by hyperphosphorylation of Akt and the mTORC1 substrate S6 during TCR activation (Figure 4A), the former of which persisted after IL-15 treatment (Figure 3C). Based on the fact that inhibition of Akt and mTORC1 during TCR activation alone rescues the IL-15 proliferation defect of the *ATM*$^{-/-}$ cells (Figures 3D and 4D), we propose that sustained activation of mTORC1 activity after TCR activation is a major defect in these cells. This is corroborated by the observed increase in phospho-S6 *in vivo* after LCMV infection (Figure 4C). Furthermore, granzyme B is activated by mTORC1 signaling,[54] and we observed increased levels of granzyme B in LCMV-infected *ATM*$^{-/-}$ mice (Figure 2C). We interpret these results to mean that one function of ATM is to integrate signals from PI3K and AMPK to properly regulate mTORC1 activity under different conditions and speculate that this may be relevant to the immunopathology in A-T. That proper balancing of PI3K/Akt signaling is needed for memory T-cell survival is likely to be salient in this regard.[55] Also, unstimulated CD8$^+$ T cells from *ATM*$^{-/-}$ mice do not exhibit hyper-Akt and mTORC1 signaling (Figure 4A), which clearly shows that this signaling defect is manifest only after TCR activation. Thus, the CD8+ T-cell proliferation and differentiation defects observed are most likely downstream effects of altered Akt/mTORC1 signaling during TCR activation. No major changes in AMPK or PTEN were observed in *ATM*$^{-/-}$ T cells before or after TCR activation (Figure 4A), but these pathways were perturbed after IL-15 treatment (Figure 3C). Thus, these are candidate downstream pathways responding to hyper-Akt/mTORC1 during TCR activation in *ATM*$^{-/-}$ CD8$^+$ T cells.

If hyperactivation of mTORC1 signaling is the primary defect in *ATM*$^{-/-}$ cells, as we concluded from our *in vitro* studies, then we reasoned that its inhibition should rescue at least some of the T-cell defects we observed *in vivo* in response to LCMV infection. Finding that rapamycin treatment during an LCMV infection significantly increased and sustained higher number of memory CD8$^+$ T cells in *ATM*$^{-/-}$ mice (Figure 5) supports this conclusion. These results are consistent with those of Araki et al,[33] who showed that inhibition of mTORC1 during early stages of LCMV infection substantially improves the quantity and quality of memory T cells in wild-type mice,[33] but our results demonstrate for the first time that this may be of therapeutic value for a specific disease state. However, we acknowledge that the rapamycin-driven increase in memory cell formation in *ATM*$^{-/-}$ mice was sustained only as long as rapamycin was being administered, and this was not maintained at later points postinfection (Figure 5). Thus a more prolonged drug regimen may be required to achieve substantial benefit or other factors/pathways are involved in addition to hyper-mTOR signaling.

At this point, we do not know the precise reason for hyperactivation of mTORC1 during TCR activation of *ATM*$^{-/-}$ CD8$^+$ T cells. Two candidates are AMPK and PTEN, which are negative regulators of mTORC1 via TSC2 and Akt, respectively;[56–58] however, AMPK and PTEN steady-state levels and phosphorylation appear normal in TCR-activated CD8$^+$ T cells (Figure 4A). Thus, in this circumstance, lack of ATM appears to lead to mTORC1 activation through phosphorylation of Akt, which is most likely by a PI3-kinase-independent mechanism. This contrasts the observation that inhibition of ATM leads to down-regulation of Akt phosphorylation during insulin signaling.[16,59] Thus, lack of ATM activity appears to have context-dependent affects on Akt phosphorylation and mTORC1 activity. This is supported by our results from IL-15 treatment of TCR-activated *ATM*$^{-/-}$ cells, which leads to increased inhibitory phosphorylation of PTEN, whereas AMPK is activated (Figure 3C). In this case, S6 phosphorylation is unaffected, which suggests that mTORC1 activity is not responding positively to up-regulation of Akt activity or negatively to up-regulation of AMPK activity. Thus, again, ATM is apparently needed to integrate inputs from multiple pathways that affect mTORC1. Consistent with this premise, ATM activation by oxidative stress regulates mTORC1 via TSC2,[21] Akt and mTORC1 are up-regulated in *ATM*$^{-/-}$ thymocytes, and rapamycin delays lymphoma formation in *ATM*$^{-/-}$ mice.[25]

In conclusion, in this study we gained greater insights into the immune system dysfunction in A-T that might aid in developing therapeutic strategies. Using the well-characterized LCMV-infection mouse model, coupled with studies of cultured splenic T cells, we found that *ATM*$^{-/-}$ mice have altered CD8$^+$ T-cell responses, defective effector-to-memory differentiation, perturbed hierarchy of T-cell epitope immunodominance, and hyperactivated Akt and mTORC1 pathways during TCR activation. The latter results in an inability of *ATM*$^{-/-}$ CD8$^+$ T cells to proliferate in response to IL-15 *in vitro*, which can be rescued by inhibition of Akt or mTORC1 during TCR stimulation. Finally, some of the memory cell defects are rescued by rapamycin treatment during LCMV infection *in vivo*, which is proof of a principle in a mouse model of the disease that targeting this pathway may be of therapeutic value for the immunopathology in A-T patients. Furthermore, if hyperactivation of Akt and/or mTORC1 results in a common molecular defect in A-T patent cells, targeting these pathways might also be of therapeutic value for the additional complex pathology of A-T.

Acknowledgments

References

1. Savitsky K, Bar-Shira A, Gilad S, Rotman G, Ziv Y, Vanagaite L, Tagle DA, Smith S, Uziel T, Sfez S, Ashkenazi M, Pecker I, Frydman M, Harnik R, Patanjali SR, Simmons A, Clines GA, Sartiel A, Gatti RA, Chessa L, Sanal O, Lavin MF, Jaspers NG, Taylor AM, Arlett CF, Miki T, Weissman SM, Lovett M, Collins FS, Shiloh Y: A single ataxia telangiectasia gene with a product similar to PI-3 kinase. Science 1995, 268:1749–1753

2. Lavin MF, Shiloh Y: The genetic defect in ataxia-telangiectasia. Annu Rev Immunol 1997, 15:177–202

3. Morrell D, Cromartie E, Swift M: Mortality and cancer incidence in 263 patients with ataxia-telangiectasia. J Natl Cancer Inst 1986, 77:89–92

4. Barlow C, Hirotsune S, Paylor R, Liyanage M, Eckhaus M, Collins F, Shiloh Y, Crawley JN, Ried T, Tagle D, Wynshaw-Boris A: Atm-deficient mice: a paradigm of ataxia telangiectasia. Cell 1996, 86:159–171

5. Elson A, Wang Y, Daugherty CJ, Morton CC, Zhou F, Campos-Torres J, Leder P: Pleiotropic defects in ataxia-telangiectasia protein-deficient mice. Proc Natl Acad Sci USA 1996, 93:13084–13089

6. Xu Y, Ashley T, Brainerd EE, Bronson RT, Meyn MS, Baltimore D: Targeted disruption of ATM leads to growth retardation, chromosomal fragmentation during meiosis, immune defects, and thymic lymphoma. Genes Dev 1996, 10:2411–2422

7. Bagley J, Cortes ML, Breakefield XO, Iacomini J: Bone marrow transplantation restores immune system function and prevents lymphoma in Atm-deficient mice. Blood 2004, 104:572–578

8. Aucouturier P, Bremard-Oury C, Griscelli C, Berthier M, Preud'homme JL: Serum IgG subclass deficiency in ataxia-telangiectasia. Clin Exp Immunol 1987, 68:392–396

9. Giovannetti A, Mazzetta F, Caprini E, Aiuti A, Marziali M, Pierdominici M, Cossarizza A, Chessa L, Scala E, Quinti I, Russo G, Fiorilli M: Skewed T-cell receptor repertoire, decreased thymic output, and predominance of terminally differentiated T cells in ataxia telangiectasia. Blood 2002, 100:4082–4089

10. Chao C, Yang EM, Xu Y: Rescue of defective T cell development and function in Atm−/− mice by a functional TCR alpha beta transgene. J Immunol 2000, 164:345–349

11. Pashankar F, Singhal V, Akabogu I, Gatti RA, Goldman FD: Intact T cell responses in ataxia telangiectasia. Clin Immunol 2006, 120:156–162

12. Rotman G, Shiloh Y: ATM: a mediator of multiple responses to genotoxic stress. Oncogene 1999, 18:6135–6144

13. Yang DQ, Kastan MB: Participation of ATM in insulin signalling through cphosphorylation of eIF-4E-binding protein 1. Nat Cell Biol 2000, 2:893–898

14. Eaton JS, Lin ZP, Sartorelli AC, Bonawitz ND, Shadel GS: Ataxia-telangiectasia mutated kinase regulates ribonucleotide reductase and mitochondrial homeostasis. J Clin Invest 2007, 117:2723–2734

15. Ambrose M, Goldstine JV, Gatti RA: Intrinsic mitochondrial dysfunction in ATM-deficient lymphoblastoid cells. Hum Mol Genet 2007, 16:2154–2164

16. Halaby MJ, Hibma JC, He J, Yang DQ: ATM protein kinase mediates full activation of Akt and regulates glucose transporter 4 translocation by insulin in muscle cells. Cell Signal 2008, 20:1555–1563

17. Suzuki A, Kusakai G, Kishimoto A, Shimojo Y, Ogura T, Lavin MF, Esumi H: IGF-1 phosphorylates AMPK-alpha subunit in ATM-dependent and LKB1-independent manner. Biochem Biophys Res Commun 2004, 324:986–992

18. Sun Y, Connors KE, Yang DQ: AICAR induces phosphorylation of AMPK in an ATM-dependent. LKB1-independent manner. Mol Cell Biochem 2007, 306:239–245

19. Fu X, Wan S, Lyu YL, Liu LF, Qi H: Etoposide induces ATM-dependent mitochondrial biogenesis through AMPK activation. PLoS One 2008, 3:e2009

20. Viniegra JG, Martinez N, Modirassari P, Losa JH, Parada Cobo C, Lobo VJ, Luquero CI, Alvarez-Vallina L, Ramon y Cajal S, Rojas JM, Sanchez-Prieto R: Full activation of PKB/Akt in response to insulin or ionizing radiation is mediated through ATM. J Biol Chem 2005, 280:4029–4036

21. Alexander A, Cai SL, Kim J, Nanez A, Sahin M, MacLean KH, Inoki K, Guan KL, Shen J, Person MD, Kusewitt D, Mills GB, Kastan MB, Walker CL: ATM signals to TSC2 in the cytoplasm to regulate mTORC1 in response to ROS. Proc Natl Acad Sci USA 2010, 107:4153–4158

22. Huang J, Dibble CC, Matsuzaki M, Manning BD: The TSC1-TSC2 complex is required for proper activation of mTOR complex 2. Mol Cell Biol 2008, 28:4104–4115

23. Zhang H, Cicchetti G, Onda H, Koon HB, Asrican K, Bajraszewski N, Vazquez F, Carpenter CL, Kwiatkowski DJ: Loss of Tsc1/Tsc2 activates mTOR and disrupts PI3K-Akt signaling through downregulation of PDGFR. J Clin Invest 2003, 112:1223–1233

24. Inoki K, Li Y, Zhu T, Wu J, Guan KL: TSC2 is phosphorylated and inhibited by Akt and suppresses mTOR signalling. Nat Cell Biol 2002, 4:648–657

25. Kuang X, Shen J, Wong PK, Yan M: Deregulation of mTOR signaling is involved in thymic lymphoma development in Atm−/− mice. Biochem Biophys Res Commun 2009, 383:368–372

26. Kaech SM, Wherry EJ, Ahmed R: Effector and memory T-cell differentiation: implications for vaccine development. Nat Rev Immunol 2002, 2:251–262

27. Parish IA, Kaech SM: Diversity in CD8(+) T cell differentiation. Curr Opin Immunol 2009, 21:291–297

28. Kaech SM, Wherry EJ: Heterogeneity and cell-fate decisions in effector and memory CD8+ T cell differentiation during viral infection. Immunity 2007, 27:393–405

29. Voehringer D, Koschella M, Pircher H: Lack of proliferative capacity of human effector and memory T cells expressing killer cell lectin-like receptor G1 (KLRG1). Blood 2002, 100:3698–3702

30. Voehringer D, Blaser C, Brawand P, Raulet DH, Hanke T, Pircher H: Viral infections induce abundant numbers of senescent CD8 T cells. J Immunol 2001, 167:4838–4843

31. Hand TW, Morre M, Kaech SM: Expression of IL-7 receptor alpha is necessary but not sufficient for the formation of memory CD8 T cells during viral infection. Proc Natl Acad Sci USA 2007, 104:11730–11735

32. Joshi NS, Cui W, Chandele A, Lee HK, Urso DR, Hagman J, Gapin L, Kaech SM: Inflammation directs memory precursor and short-lived effector CD8(+) T cell fates via the graded expression of T-bet transcription factor. Immunity 2007, 27:281–295

33. Araki K, Turner AP, Shaffer VO, Gangappa S, Keller SA, Bachmann MF, Larsen CP, Ahmed R: mTOR regulates memory CD8 T-cell differentiation. Nature 2009, 460:108–112

34. Schluns KS, Lefrancois L: Cytokine control of memory T-cell development and survival. Nat Rev Immunol 2003, 3:269–279

35. Tamas P, Hawley SA, Clarke RG, Mustard KJ, Green K, Hardie DG, Cantrell DA: Regulation of the energy sensor AMP-activated protein kinase by antigen receptor and Ca2+ in T lymphocytes. J Exp Med 2006, 203:1665–1670

36. D'Souza AD, Parikh N, Kaech SM, Shadel GS: Convergence of multiple signaling pathways is required to coordinately up-regulate mtDNA and mitochondrial biogenesis during T cell activation. Mitochondrion 2007, 7:374–385

37. Pearce EL, Walsh MC, Cejas PJ, Harms GM, Shen H, Wang LS, Jones RG, Choi Y: Enhancing CD8 T-cell memory by modulating fatty acid metabolism. Nature 2009, 460:103–107

38. Delgoffe GM, Kole TP, Zheng Y, Zarek PE, Matthews KL, Xiao B, Worley PF, Kozma SC, Powell JD: The mTOR kinase differentially regulates effector and regulatory T cell lineage commitment. Immunity 2009, 30:832–844

39. Rao RR, Li Q, Odunsi K, Shrikant PA: The mTOR kinase determines effector versus memory CD8+ T cell fate by regulating the expression of transcription factors T-bet and Eomesodermin. Immunity 2010, 32:67–78

40. Kaech SM, Tan JT, Wherry EJ, Konieczny BT, Surh CD, Ahmed R: Selective expression of the interleukin 7 receptor identifies effector CD8 T cells that give rise to long-lived memory cells. Nat Immunol 2003, 4:1191–1198

41. Wherry EJ, Teichgraber V, Becker TC, Masopust D, Kaech SM, Antia R, von Andrian UH, Ahmed R: Lineage relationship and protective immunity of memory CD8 T cell subsets. Nat Immunol 2003, 4:225–234

42. Chandele A, Joshi NS, Zhu J, Paul WE, Leonard WJ, Kaech SM: Formation of IL-7Ralphahigh and IL-7Ralphalow CD8 T cells during infection is regulated by the opposing functions of GABPalpha and Gfi-1. J Immunol 2008, 180:5309–5319

43. Sallusto F, Lenig D, Forster R, Lipp M, Lanzavecchia A: Two subsets of memory T lymphocytes with distinct homing potentials and effector functions. Nature 1999, 401:708–712

44. Weninger W, Crowley MA, Manjunath N, von Andrian UH: Migratory properties of naive, effector, and memory CD8(+) T cells. J Exp Med 2001, 194:953–966

45. Cornish GH, Sinclair LV, Cantrell DA: Differential regulation of T-cell growth by IL-2 and IL-15. Blood 2006, 108:600–608

46. Becker TC, Wherry EJ, Boone D, Murali-Krishna K, Antia R, Ma A, Ahmed R: Interleukin 15 is required for proliferative renewal of virus-specific memory CD8 T cells. J Exp Med 2002, 195:1541–1548

47. Wherry EJ, Becker TC, Boone D, Kaja MK, Ma A, Ahmed R: Homeostatic proliferation but not the generation of virus specific memory CD8 T cells is impaired in the absence of IL-15 or IL-15Ralpha. Adv Exp Med Biol 2002, 512:165–175

48. Kalia V, Sarkar S, Subramaniam S, Haining WN, Smith KA, Ahmed R: Prolonged interleukin-2Ralpha expression on virus-specific CD8+ T cells favors terminal-effector differentiation in vivo. Immunity 2010, 32:91–103

49. Hand TW, Kaech SM: Intrinsic and extrinsic control of effector T cell survival and memory T cell development. Immunol Res 2009, 45:46–61

50. Schubert R, Reichenbach J, Zielen S: Deficiencies in CD4+ and CD8+ T cell subsets in ataxia telangiectasia. Clin Exp Immunol 2002, 129:125–132

51. Miles PD, Treuner K, Latronica M, Olefsky JM, Barlow C: Impaired insulin secretion in a mouse model of ataxia telangiectasia. Am J Physiol Endocrinol Metab 2007, 293:E70–E74

52. Westbrook AM, Schiestl RH: Atm-deficient mice exhibit increased sensitivity to dextran sulfate sodium-induced colitis characterized by elevated DNA damage and persistent immune activation. Cancer Res 2010, 70:1875–1884

53. Raue HP, Slifka MK: CD8+ T cell immunodominance shifts during the early stages of acute LCMV infection independently from functional avidity maturation. Virology 2009, 390:197–204

54. Efimova OV, Kelley TW: Induction of granzyme B expression in T-cell receptor/CD28-stimulated human regulatory T cells is suppressed by inhibitors of the PI3K-mTOR pathway. BMC Immunol 2009, 10:59

55. Hand TW, Cui W, Jung YW, Sefik E, Joshi NS, Chandele A, Liu Y, Kaech SM: Differential effects of STAT5 and PI3K/AKT signaling on effector and memory CD8 T-cell survival. Proc Natl Acad Sci USA 2010, 107:16601–16606

56. Chalhoub N, Baker SJ: PTEN and the PI3-kinase pathway in cancer. Annu Rev Pathol 2009, 4:127–150

57. Gwinn DM, Shackelford DB, Egan DF, Mihaylova MM, Mery A, Vasquez DS, Turk BE, Shaw RJ: AMPK phosphorylation of raptor mediates a metabolic checkpoint. Mol Cell 2008, 30:214–226

58. Inoki K, Zhu T, Guan KL: TSC2 mediates cellular energy response to control cell growth and survival. Cell 2003, 115:577–590

59. Li Y, Yang DQ: The ATM inhibitor KU-55933 suppresses cell proliferation and induces apoptosis by blocking Akt in cancer cells with overactivated Akt. Mol Cancer Ther 2010, 9:113–125